Eur Respir J, 1994, 7, 1409–1415
DOI: 10.1183/09031936.94.07081409

European Respiratory Journals
ISSN 0903 - 1936

A comparison between the epithelial tight junction morphology of human extrapulmonary bronchi and rat trachea

R.W.A. Godfrey*, N.J. Severs**, P.K. Jeffery*

A comparison between the epithelial tight junction morphology of human extrapulmonary bronchi and rat trachea. R.W.A. Godfrey, N.J. Severs, P.K. Jeffery. ©ERS Journals Ltd 1994.

ABSTRACT: Animal models have been used to investigate the involvement of epithelial tight junctions in the pathogenesis of human airway disease. However, no previous study has compared the tight junction morphologies of human and animal species in order to relate findings in animal models to human disease. In the present study, we therefore undertook a comprehensive quantitative evaluation of tight junction morphology, to determine what similarities or differences may exist in rat and human airways.

Human tissue was obtained from grossly and histologically normal extrapulmonary bronchi from lungs resected for pulmonary tumour (n=8); rat tracheal epithelium was acquired from Sprague-Dawley specific pathogen-free animals (n=12). The tight junction morphologies of the two species were compared with respect to junctional depth, number of strands and junctional complexity.

The basic architectural arrangement of the tight junctions in both species was found to be similar; however, tight junctions in rat tissues were less deep, comprised fewer strands, and had fewer strand interconnections compared with those in the human samples. The number of strands per interconnection was similar in the two species.

We conclude that, in spite of a general similarity of rat and human airway epithelial tight junctions, there are specific quantitative details of morphology which need to be considered when attempting to extrapolate to the human the results of studies of airway epithelial permeability conducted in the rat. The precise biological significance of these differences, as yet, remains unclear.
Eur Respir J, 1994, 7, 1409–1415.

Depts of *Lung Pathology and **Cardiac Medicine, Royal Brompton National Heart and Lung Institute, London, UK.

Correspondence: P.K. Jeffery
Dept of Lung Pathology
Royal Brompton National Heart and Lung Institute
Sydney Street
London SW3 6NP
UK

Keywords: Airways
human
rat
tight junctions

Received: June 29 1993
Accepted after revision April 16 1994

This work was supported by the Wellcome Trust (UK), Grant number: 034612/Z/91/Z/1.5.

Studies on rodents have played a major part in advancing our understanding of the structure and function of normal mammalian airways [1], and nonprimate animal models have been successfully developed for the investigation of the pathogenesis of airway disease [2–8]. The specific pathogen-free rat, following exposure to a variety of inhaled irritants, has been widely used to model human chronic bronchitis: the response to irritation includes a thickening of airway epithelium, goblet cell hyperplasia, increased production of mucus and increased epithelial permeability [4, 9–11]. The possible beneficial effects of a number of distinct classes of drug has also been studied using this model [12–16]. Interestingly, the study of the relationship between irritant-induced increased epithelial permeability and tight junction structure has produced inconsistent results [17–22].

Freeze-fracture electron microscopy reveals details of tight junction morphology *en face* [23–27], and methods to quantify tight junction ultrastructure using this technique have been developed [27, 28]. Comparative data on nasal epithelia in a number of nonprimate species have been published [28], but comparisons between nonprimate and a primate epithelia of the lower respiratory tract are lacking. No comprehensive quantitative comparison of human and rat airway epithelial tight junctions has previously been undertaken, even though the rat has been widely used to model human airway disease. Such a study is needed to justify the use of the rat as a model system for studies of airway permeability, the results of which are often extrapolated to humans.

The present study set out to compare, by quantitative methods, the tight junction morphologies of extrapulmonary airway epithelia of rat and humans. Our objectives were to determine whether structural differences exist between these species, to determine the extent of inter- and intra-individual variation, and, thereby, to assist in the interpretation of data from animal models used for the investigation of tight junction structure in relation to epithelial permeability in health and disease. The structural components of the tight junction analysed included: 1) junctional depth; 2) number of strands across the belt; and 3) the complexity of the junction.

Materials and methods

Preparation of material and freeze-fracture

Human tissue was obtained from grossly normal extrapulmonary bronchi taken distant from circumscribed tumour in lungs resected for pulmonary tumour (n=8; 4

male and 4 female; age range 18–67 yrs; 6 ex-smokers and 2 nonsmoker) [27]. Portions of main bronchus and/or lobar bronchus were examined. For comparison, tracheal epithelium was obtained from 12 cage control specific Sprague-Dawley rats; Charles Rivers Ltd, London, UK). The absence of epithelial atypia both in the human and animal samples was confirmed by histological examination.

Transversely cut rings of airway were prepared for histology, and for thin section and freeze-fracture electron microscopy. All tissue for electron microscopy was initially fixed in 3% glutaraldehyde in sodium cacodylate buffer (0.1 M pH 7.4 at 4°C) and fixed for a period of 2–36 h. In the case of the human tissue, transversely cut rings of airway were placed in fixative within 30 min of resection. The rat tissue was fixed *in situ* using the system previously developed in our laboratory to perfuse animal tracheae with physiological saline solution [6]. For freeze-fracture, the fixed tissue was transferred into 30% glycerol in cacodylate buffer and stored overnight at 4°C. Each bronchial or tracheal ring was then divided longitudinally and the epithelium separated gently from the underlying mucosa using a sharp scalpel. Epithelial strips were mounted in standard gold alloy holders (Balzers High Vacuum Ltd, Milton Keynes, UK), with approximately 1 mm of the sample projecting. The samples were frozen by plunging them into liquid nitrogen-cooled Freon ("Arcton 12" ICI Runcorn, Cheshire, UK) and each was subsequently stored under liquid nitrogen until processing for freeze-fracture replication.

Freeze-fracture replicas were prepared in a Balzers BAF 400T freeze-fracture apparatus. Fracturing was carried out by knife at a temperature of -115°C with a vacuum greater than 10^{-6} mbar. Standard unidirectionally-shadowed platinum-carbon replicas were prepared, and cleaned using sodium hypochlorite. The replicas were mounted and viewed in a Philips EM 301 electron microscope.

Quantification

Freeze-fracture replicas were prepared from a minimum of six samples from each subject. All the junctions observed were routinely photographed, and printed to a final magnification of ×90,000. Those junctions occurring on areas of steeply inclined membrane were excluded from the analysis. Even with this approach, not all of the membranes were precisely horizontal owing to natural curvature of the cell. However, as this affects absolute values randomly in all four groups, it does not bias the results of the comparative study in favour of any one group. One hundred and seventy three micrographs were analysed from human airways, corresponding to a total tight junctional length of 195 μm. For the rat, 79 micrographs were analysed, giving a total length of 87 μm.

Figure 1 explains the approach to quantification. Vertical lines were drawn at 5 cm intervals (equivalent to junctional lengths of 555 nm) perpendicular to a line projected along the luminal edge of each tight junction. The depth of the junction (*i.e.* the overall width of the belt of strands/grooves) was measured on each vertical grid line using the quantitative system described previously [23]. The same grid lines were used to count the number of strands comprising the junctional belt, in an apical/basal direction. Junctional complexity was assessed using the sampling areas defined by the grid lines. In these areas, the total length of junctional strand/groove in each alternate sampling area was measured using an Apple Macintosh image analysis system (Improvision Ltd, Coventry UK), and the number of interconnections counted. Using these data, the number of interconnections per μm length of strand was calculated. The interconnections were then classified into those involving 3, 4, 5 and 6 strands, and the number falling into each category was expressed as a percentage.

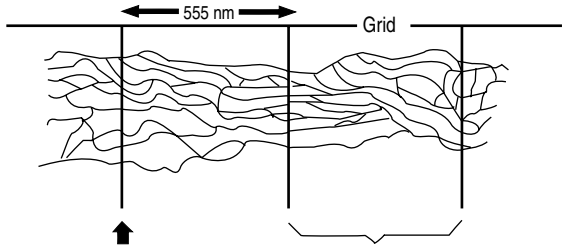

Fig. 1. – Diagrammatic representation of tight junction morphology illustrating our approach to quantitative analysis. A grid line was drawn parallel to the luminal edge of each junction. Vertical lines, drawn at intervals of 555 nm from this horizontal line, were used to count the number of strands across the belt and to measure the depth (belt width) of the junction. In the areas defined by the grid lines, the total length of junction strands was measured and the number of interconnections between strands determined. From these data, the number of interconnections per μm length of strand was calculated. Interconnections were also classified into those involving 3, 4, 5 or 6 strands, and the number in each category was recorded. 1) and 2) were measured on every vertical grid line. 3), 4) and 5) were determined on every alternate grid area.

Comparisons between the groups were made using the Student's t-test, the Mann-Whitney U-test, or the Chi-squared test, as appropriate [29].

Results

General morphology

Freeze-fracture replicas of the human and rat airway epithelium revealed details of the pseudostratified layer of cells previously well characterized by thin-section electron microscopy [30, 31]. Among the cell types recognized were ciliated cells, possessing cilia, filiform microvilli and apically-located mitochondria; and secretory cells, containing either small discrete granules or larger more confluent (mucous) granules and typically short micro-villi. In addition, there were cells of indeterminate phenotype with numerous microvilli covering their apical surfaces [27].

Fig. 2. – Electron micrograph illustrating a tight junction found in normal human airways. The tight junction belt (B) is clearly organized in a zone at the cell apex, Intramembrane particles, microvilli (M), and a typical tricellular junctional arrangement (T) are visible. The view is predominantly of the P face of plasma membranes. (For details of fracture face terminology, see BRANTON [32] *et al*. 1975). The identities of the participating cells cannot be determined with certainty in this freeze-fracture view. Short arrow indicates direction of shadowing. (Bar=1 μm).

The freeze-fractured tight junctions of both the human and rat airway epithelium revealed the usual series of interconnecting strands (fibrils) on the P-face and complementary grooves on the E-face, arranged in belt-form around the apicolateral borders of the superficial epithelial cell layer (figs 2–6). Within this basic architectural arrangement, a wide variation in the morphological features of the individual tight junctions was evident; strand number, total depth of the junctional belt, and frequency and complexity of strand interconnection being the most prominent and variable features (fig. 3). Both "Parallel" forms, (*i.e*. junctions comprising parallel strands and few interconnections figs 3b and 4), and "network" forms (with numerous strand interconnections (fig. 2) were both regularly encountered, as were numerous intermediate morphologies between these two extremes (fig. 5). While strand interconnection was often uniform throughout the depth of the belt on the basal aspect, many junctions tended to show a looser meshwork, with either free-ended strands and/or loops which remained continuous with the main belt (figs 2 and 6). These abluminal loops were more common in tight junctions obtained from rat airways than in those obtained from human airways. Tricellular regions, extending basally beyond the apical belt, were occasionally detected both in human and rat airways.

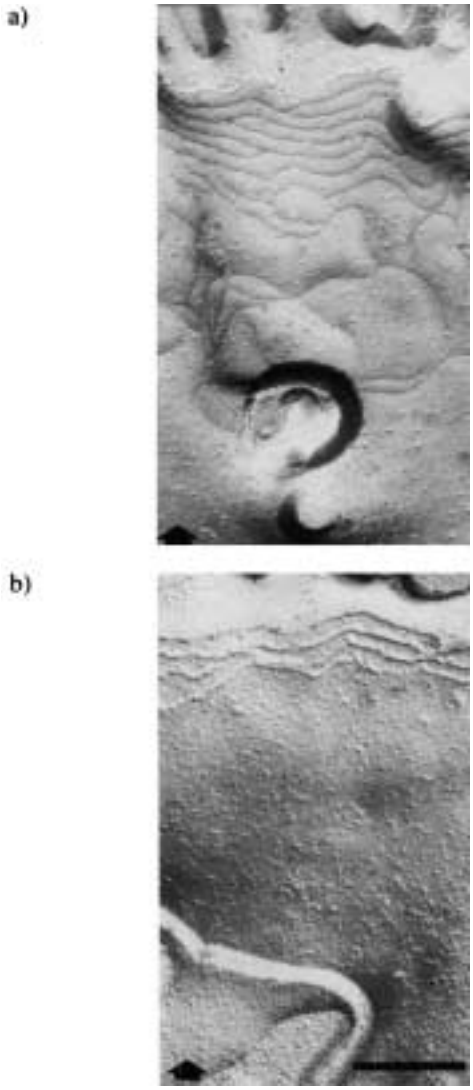

Fig. 3. – Variation in tight junction morphology found in control rat trachea. These examples illustrate how belt depth (width) and strand number vary from one junction to the next. a) Shows a belt-like tight junctional network, detected immediately underneath the luminal surface associated with a ciliated cell composed of approximately 12 strands. b) Shows a narrow junction composed of 4 strands. Both examples come from junctions between a ciliated cell and a cell of indeterminate phenotype, seen in P-face views. Short arrow indicated direction of shadowing. (Bar=250 nm).

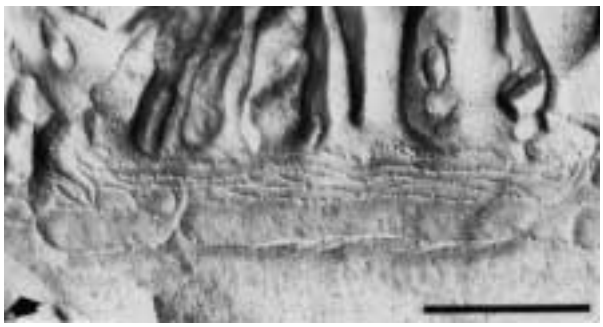

Fig. 4. – An example from a control rat trachea. P-face of a tight junction associated with a ciliated cell consisting of parallel strands with a few interconnections and abluminal basal loops. Short arrow indicates direction of shadowing. (Bar=500 nm).

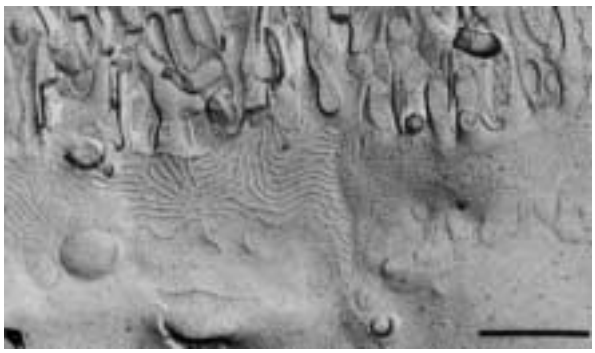

Fig. 5. – A tight junctional expanse containing a tricellular region from a human bronchial airway. The view is predominantly of the P-face to the left of the micrograph and the E-face to the right of the micrograph. The tight junction illustrated is between two cells of indeterminate cell type. Short arrow indicates direction of shadowing. (Bar=500 nm).

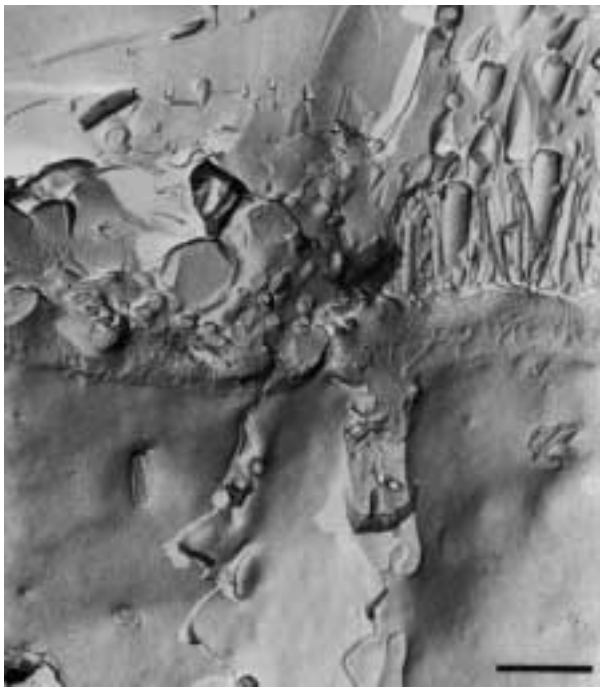

Fig. 6. – Electron micrograph illustrating a tight junctional expanse from normal human airways. Note there is little variation in junctional morphology in terms of junction depth strand number and complexity between the tight junction on the left of the micrograph (between an "actively secreting" mucous cell and a cell of indeterminate phenotype) and the junction on the left of the micrograph (between a ciliated cell and a cell of indeterminate phenotype). Short arrow indicates direction of shadowing. (Bar=1 μm).

Quantitative comparison between the tight junction morphology of normal human and control rat airways

Table 1 summarizes the data on junction depth, number of strands vertically across the belt, and the number of interconnections per μm strand in the two species. Histograms depicting the frequency distributions of these morphological features showed that these data, both in rat and human airways, were normally distributed.

Mean junctional depth was significantly greater in the human airways than in the rat ($p<0.001$). The average coefficients of variation within a given individual of a group were 9.9% in the case of human airways and 15.5% for rat airways, whilst the values between individuals in a group were 31.0 and 33.8%, respectively.

Table 1. – Measurements of tight junction in human and rat airways

	Junctional depth μm	Strands n	Interconnections per μm strand n
Human bronchi	0.47** (0.13)	10.90** (0.10)	1.40** (0.04)
Rat trachea	0.35 (0.01)	8.00 (0.20)	0.83 (0.05)

Data are presented as mean (SEM). **: $p<0.001$ human *vs* rat (Student's t-test).

Strand number ranged 4–26 in the human airways and 5–13 in the rat; the data in both species showing a normal distribution. The difference in strand number between the two groups was statistically significant ($p<0.001$). The average coefficients of variation within a given individual of a group were 4.2% for the human bronchi and 11.1% for the rat tracheal airways. The coefficients of variation between individuals in a group were 25.2 and 19.4%, respectively.

The number of interconnections per μm of junctional strand ranged 0.6–2.45 in the human airways and 0.36–1.49 in the rat airways. The difference between the two species was statistically significant ($p<0.001$). The coefficients of variation within a given individual of a group were 14.5% for human airways and 22.5% for rat; the values for the variation between individuals were 23.8 and 20.5%, respectively.

In both species, the most common form of interconnection involved the joining of 3 junctional strands; the most ever found was 6 in the case of the human airways and 5 in the rat (table 2). However, the difference between the mean of the two species was not significant statistically (Chi-squared test). Histograms comparing frequency distributions for this parameter showed that the data were not normally distributed but followed a J-shaped distribution pattern [29]. The coefficients of variation between individuals or animals for 3 strands meeting was 1.3% in the case of human airways and 3.8% in the case of rat airways. The corresponding values for 4 strands meeting were 15.6 and 13.3%, respectively. The increase in values of the coefficient of variation for joins involving 4 strands compared with those involving 3 strands reflects the infrequency of interconnections involving 4 or more strands.

Discussion

In the present study, we decided to focus on the specific pathogen-free rat for comparison with human airways, as this animal species has frequently been used

Table 2. – Tight junction strand interconnection frequency (%) in human and rat airways

	Number of strands meeting at each interconnection			
	3	4	5	6
Human bronchi	83.2 (1.2)	15.4 (1.3)	1.1 (0.2)	0.2 (0.04)
Rat trachea	78.9 (3.0)	18.3 (2.5)	2.1 (0.7)	0

Interconnections between strands of a tight junction may involve the meeting of 3, 4, 5 or 6 strands. Frequencies, expressed as a percentage of total number examined, of each of these categories of interconnection, (SEM) are shown.

to model the irritant-induced changes seen in human in chronic bronchitis: *i.e.* a thickening of the epithelium, goblet cell hyperplasia, and increase in mucus production coupled with a shift to the production of a more acidic mucus [4, 9–11]. Whilst architecturally similar, the bronchial tight-junctional belt in the extrapulmonary bronchi of humans appeared to be deeper and more complex than those observed in the rat trachea. In human bronchial junctions, the number of strands comprising the belt was approximately 11, the belt extended to an average depth of 0.46 μm, and the average number of interconnections per μm strand length was 1.4. The corresponding values for the rat trachea were 8, 0.25 μm and 0.8, respectively, ($p<0.001$ for all three parameters). There were no statistical differences between the two groups for the number of junctional strands meeting at each interconnection. These differences of magnitude may have functional implications.

The characteristic structure of the tight junction, revealed as a series of interwoven intramembrane strands or fibrils in planar freeze-fracture view, is well-established [33]. The number of strands comprising the tight junction belt is thought to be one factor controlling permeability of the epithelial paracellular pathway to ions, water and macromolecules [34]. Selective permeability of the tight junction to these molecules, together with active translocation of ions, results in the generation of a transepithelial potential difference. The association of junctional morphology and trans-epithelial electrical resistance has been determined, and an equation derived which relates the two [35]. A number of independent studies conducted both in animals and humans have shown that the transepithelial potential difference becomes less lumen-negative distally in the airways than proximally [36–38]. Applying the "count strand hypothesis" of CLAUDE [35] to these data, the structure of the tight junctions in the trachea of a given animal would be predicted to be deeper and more complex than that of the main and lobar bronchi. However, as we found human bronchial tight junctions to be more complex than those of the rat trachea, any effect of the difference of airway size would tend to reduce, rather than accentuate, the structural differences in the comparison made in the present study.

Interestingly, BOUCHER *et al.* [36] reported that the potential difference obtained *in vivo* from guinea-pig airways was significantly less than that obtained from rat airways (tracheal values of 7.8 mV for the guinea-pig compared to 13.8 mV for the rat). These results are reflected in the observation that tight junctions in the guinea-pig tracheal epithelium were reported to consist of up to 7 interconnecting strands [39], whilst in the rat tracheal airways sampled in the present study the maximum number of strands comprising a junction was 14, with an average of approximately 8. Three distinct junctional types were reported in rat tracheal airways by SCHNEEBERGER [26], the most common and complex being found between ciliated cells (*i.e.* 5–12 strands with a mean number of 7 strands).

BOUCHER *et al.* [36] have also reported high lumen-negative potential difference in dog trachea and bronchi, the values being approximately twice those reported for the rat (28.5 mV in the case of dog trachea and 13.8 mV in the rat). However, the physiological results may not be reflected in differences in strand number or density between the species, as MENCO [28] has reported similar values for strand number in rat and dog nasal epithelium. A possible explanation for this apparent discrepancy is that the mechanisms underlying epithelial ion transport movement differ in these two species: the dog trachea exhibits a baseline or resting net secretion of chloride ions into the airway, whilst the rat trachea exhibits a baseline net absorption of sodium ions from the luminal surface [40].

The present study has established by quantification the structural characteristics of epithelial tight junctions found in "normal" human and rat airways. An important consideration is the large magnitude of intra- and interindividual variation in the parameters quantified: *e.g.* junctional depth both in human and rat airways has a between-individual coefficient of variation up to 34%. Furthermore, considerable variation in strand arrangement is apparent from one junction to the next and within a junction of a single cell: both the parallel and network stranding patterns are evident, with numerous examples of gradations between these two forms. When designing quantitative experiments to investigate tight junction morphology, this inherent, sometimes substantial, variation should clearly be taken into account and samples of appropriate size analysed.

The major functions of the airway epithelium in humans and rat may be regarded as similar; both are comprised of pseudostratified epithelia, which have in common a number of cell types and show broadly similar transepithelial electrical properties [1, 36–38, 40]. However, there are distinct structural variations in microstructure and anatomy: for example in cell type, shape and height. Surface epithelial serous cells are found in the extrapulmonary specific pathogen-free rat airways, but in adult human airways they are restricted to the bronchioli [30, 41]. In human bronchial epithelium, the cells are predominately columnar in shape and approximately 50 μm in height, whereas in the rat mid/ lower trachea and bronchi the cells are more cubodial in shape and are smaller, *i.e.* the epithelium is

approximately 12 μm in height [5, 30, 42]. Moreover, airway diameter varies in direct proportion to the size of the animal [43], and the force needed to deform (expand) a small airway is likely to be significantly greater than that required for a larger airway [44]. All these features of distinction between the two species may potentially influence cell-to-cell interaction and the complexity of tight junction morphology.

In conclusion, the rat and human airways share many common structural and functional features. Despite this overall similarity, the technique of freeze-fracture, which can detect subtle changes in tight junction morphology, has demonstrated quantitative differences in some structural features of the junctions between the two species. These differences and the baseline structural similarities need to be considered when attempting to extrapolate the results of experimental studies of airway permeability in the rat to those of man.

Acknowledgements: The authors gratefully acknowledge the expert technical assistance of S. Rothery.

References

1. Jeffery PK. Morphological features of airway epithelial cells and glands. *Am Rev Respir Dis* 1983; 129: S14–20.
2. Reid L. An experimental study of hypersecretion of mucus in the bronchial tree. *Br J Exp Path* 1963; 44: 437–445.
3. Reid L. Evaluation of model systems for the study of airway epithelium, cilia and mucus. *Arch Intern Med* 1970; 126: 426–434.
4. Lamb D, Reid L. Mitotic rates, goblet cell increase and histochemical changes in rat bronchial epithelium during exposure to sulphur dioxide. *J Pathol Bacteriol* 1986; 96: 97–111.
5. Jeffery PK, Reid L. The effect of tobacco smoke, with or without phenylmethyloxadiazole (PMO), on rat bronchial epithelium: a light and electron microscopic study. *J Pathol* 1981; 133: 341–351.
6. Rogers DF, Turner NC, Marriot C, Jeffery PK. Cigarette smoke-induced "chronic bronchitis" a study *in situ* of laryngotracheal hypersecretion in the rat. *Clin Sci* 1987; 72: 629–637.
7. Christensen TG, Korthy AL, Snider GL, Hayes JA. Irreversible bronchial goblet cell metaplasia in hamsters with elastase-induced panacinar emphysema. *J Clin Invest* 1977; 59: 397–404.
8. Huber GL, Davies P, Zwilling GR, *et al.* A morphologic and physiologic bioassay for quantifying alterations in the lung following experimental chronic inhalation of tobacco smoke. *Bull Eur Physiopathol Respir* 1981; 17: 269–327.
9. Jones R, Bolduc P, Reid L. Goblet cell glycoprotein and tracheal gland hypertrophy in rat airways: the effect of tobacco smoke with or without the anti-inflammatory agent phenylmethyloxadiazole. *Br J Exp Path* 1973; 54: 229–232.
10. Hayashi M, Sornberger C, Huber GL. Differential response in the male and; female tracheal epithelium following exposure to tobacco smoke. *Chest* 1978; 73: 515–518.
11. Huber GL, Davies P, Zwilling GR, *et al.* A morphological and physiological bioassay for quantifying alterations in the lung following experimental chronic inhalation of tobacco smoke. *Bull Eur Physiopathol Respir* 1981; 17: 269–327.
12. Jeffery PK, Rogers DF, Ayers MN. Effect of oral-acetylcysteine on tobacco smoke-induced secretory cell hyperplasia. *Eur J Respir Dis* 1985; 66: 117–122.
13. Rogers DF, Jeffery PK. Inhibition of oral N-acetylcysteine of cigarette smoke-induced chronic bronchitis in the rat. *Exp Lung Res* 1986; 10: 267–283.
14. Rogers DF, Jeffery PK. Inhibition of cigarette smoke-induced airway secretory cell hyperplasia by indomethacin, dexamethasone, prednisolone or hydrocortisone in the rat. *Exp Lung Res* 1986; 10: 285–295.
15. Rogers DF, Jeffery PK. Indomethacin and flurbiprofen speed recovery of rat bronchial epithelium after exposure to cigarette smoke. *Exp Lung Res* 1986; 10: 229–312.
16. Rogers DF, Turner NC, Marriott C, Jeffery PK. N-acetylcysteine or S-carboxymethylcysteine inhibit cigarette smoke-induced hypersecretion of mucus in rat larynx and trachea *in situ*. *Eur Respir J* 1989; 2: 955–960.
17. Simani AS, Inoue S, Hogg JC. Penetration of the respiratory epithelium of guinea-pigs following exposure to cigarette smoke. *Lab Invest* 1974; 31: 75–81.
18. Boucher RC, Johnson J, Inoue S, Hulbert W, Hogg JC. The effect of cigarette smoke on the permeability of guinea-pig airways. *Lab Invest* 1980a; 43: 94–100.
19. Hulbert WC, Walker DC, Jackson A, Hogg JC. Airway permeabilty to horseradish peroxidase in guinea-pigs: the repair phase after injury by cigarette smoke. *Am Rev Respir Dis* 1981; 123: 320–326.
20. Walker DC, Mac Kenzie A, Wiggs BR, Hulbert WC, Hogg JC. The structure of tight junctions may not correlate with permeabilty. *Cell Tissue Res* 1984; 235: 607–613.
21. Walker DC, MacKenzie A, Hulbert WC, Hogg JC. A reassessment of the tricellular region of epithelial cell tight junctions in guinea-pigs. *Acta Anat* 1985; 122: 35–38.
22. Gordon RE, Solano D, Kleinerman J. Tight junction alterations of respiratory epithelium following long-term nitrogen dioxide exposure and recovery. *Exp Lung Res* 1986; 11: 179–193.
23. Matsumura H, Setoguti T. Freeze-fracture replica studies of tight junctions in normal human bronchial epithelium. *Acta Anat Basal* 1989; 134: 219–226.
24. Elia C, Bucca C, Rolla G, Scappaticci E, Cantino D. A freeze-fracture study of the human bronchial epithelium in normal, bronchitic and asthmatic subjects. *J Submicrosc Cytol Pathol* 1988; 20: 509–511.
25. Carson JL, Collier AM, Knowles MR, Boucher RC. Ultrastructural characterization of epithelial cell membranes in normal human conducting airway epithelium: a freeze-fracture study. *Am J Anat* 1985; 173: 257–268.
26. Schneeberger EE. Heterogeneity of tight junction morphology in extrapulmonary and intrapulmonary airways in the rat. *Anat Rec* 1980; 198: 193–203.
27. Godfrey RWA, Severs NJ, Jeffery PK. Freeze-fracture morphology and quantification of human bronchial epithelial tight junctions. *Am J Respir Cell Mol Biol* 1992; 6: 453–458.
28. Menco BPM. Qualitative and quantitative freeze-fracture studies on olfactory and nasal epithelial surfaces of frog, ox, rat and dog. III. Tight junctions. *Cell Tissue Res* 1980; 211: 361–373.

29. Bland M. *In*: An Introduction to Medical Statistics. Oxford, Oxford Medical Publications, 1987.
30. Jeffery PK, Reid L. New observations of rat airway epithelium: a quantitative and electron microscopic study. *J Anat* 1975; 120: 295–320.
31. Jeffery PK. Microscopic structure of normal lung. *In*: Brewis RA, Gibson GJ, Geddes DM, eds. Textbook of Respiratory Medicine. London, Balliere Tindall, 1990; pp. 57–78.
32. Branton D, Bullivant S, Gillula NB, *et al*. Freeze-etching momenclature. *Science* 1975; 190: 54–56.
33. Gumbiner B. Structure, biochemistry and assembly of tight junctions. *Am Phys Soc* 1987; 253: C749–C758.
34. Claude P, Goodenough DA. Fracture faces of zonula occludentes from tight and leaky epithelia. *J Cell Biol* 1973; 58: 390–400.
35. Claude P. Morphological factors influencing transepithelial permeability: a model for the resistance of the zonula occludens. *J Membr Biol* 1978; 39: 219–232.
36. Boucher RC, Bromberg PA, Gatzy JT. Airway transepithelial electric potential difference *in vivo*: species and regional differences. *Am Phys Soc* 1980b; 48: 169–176.
37. Knowles MR, Carson JL, Collier AM, Gatzy JT, Boucher RC. Measurements of nasal transepithelial potential differences in normal human subjects *in vivo*. *Am Rev Respir Dis* 1981; 124: 484–490.
38. Alton EWFW, Khagani A, Taylor RFH, Logan-Sinclair R, Yacoub M, Geddes DM. Effect of heart-lung transplantation on airway potential difference in patients with and without cystic fibrosis. *Eur Respir J* 1991; 4: 5–9.
39. Inoue S, Hogg JC. Freeze-etch study of the tracheal epithelium of normal guinea-pigs with particular reference to intercellular junctions. *J Ultrastruct Res* 1977; 61: 89–99.
40. Boucher RC, Narvarte J, Cotton C, *et al*. Sodium absorption in mammalian airways. *In*: Martinez JR, Hopper U, eds. Fluid and Electrolyte Abnormalities in Exocrine Glands in CF. USA, San Francisco Press, 1982; pp. 271–287.
41. Rogers AV, Dewar A, Corrin B, Jeffery PK. Identification of serous-like cells in the surface epithelium of human bronchioles. *Eur Respir J* 1993; 6: 498–504.
42. Evans MJ, Plopper CG. The role of basal cells in adhesion of columnar epithelium to airway basement membrane. *Am Rev Respir Dis* 1988; 138: 481–483.
43. Weibel ER, Taylor CR. Design of the mammalian respiratory system. *Respir Physiol* 1981; 44: 1–164.
44. Nunn JF. Elastic forces and lung volumes. *In*: Nunn JF, ed. Applied Respiratory Physiology. 3rd edn. Cambridge, UK, Butterworths, University Press, 1987; pp. 23–45.